EPJ Web of Conferences **260**, 05002 (2022) https://doi.org/10.1051/epjconf/202226005002
NIC-XVI

Effects of Nuclear Equation of State on Type-I X-ray Bursts and Implication for *Clocked Burster* GS 1826–24

Akira Dohi[1,2,*], *Nobuya* Nishimura[3,4], *Masa-aki* Hashimoto[1], *Yasuhide* Matsuo[1], *Tsuneo* Noda[5], and *Shigehiro* Nagataki[3]

[1]Department of Physics, Kyushu University, Fukuoka 819-0395, Japan
[2]Interdisciplinary Theoretical and Mathematical Sciences Program (iTHEMS), RIKEN, Wako, Saitama 351-0198, Japan
[3]Astrophysical Big Bang Laboratory, CPR, RIKEN, Wako, Saitama 351-0198, Japan
[4]RIKEN Nishina Center for Accelerator-Based Science, Wako, Saitama 351-0198, Japan
[5]Department of Education and Creation Engineering, Kurume Institute of Technology, Kurume, Fukuoka 830-0052, Japan

Abstract. We study the effects of nuclear equation of state (EOS) on Type-I X-ray bursts, focusing on the *Clocked burster* GS 1826–24. According to the *shell-flush* model, the surface gravity of the neutron stars (NSs) strengthens burst activities, where the recurrence time and peak luminosity are higher for larger-radius EOSs. We show that such a prediction matches with the *full* multi-zone model, in which whole NS regions are considered in burst calculation. We also show that the large-radius EOSs are not preferred to account for the observed light curves of GS 1826–24.

1 Introduction

Type-I X-ray bursts, which are caused by unstable H or He burning onto a neutron star (NS), are valuable phenomena to understand the various properties of X-ray binaries such as the accretion rate, compositions of accreted matter, and nuclear reaction rates relevant to the rp process. Few observed bursters show the constant shape of light curves in a burst sequence. They are called clocked bursters, which are useful for constraining the model parameters of low-mass X-ray binaries. Several works have been done for modeling of a representative clocked burster, GS 1826–24, and finally constrained model parameters. These studies, however, mostly focused on the outer layers of the NS (e.g., [1]).

The physical properties inside the NS, such as the nuclear equation of state (EOS), crustal heating, and neutrino cooling processes, can affect the X-ray-burst light curves. Thanks to the recent developments of NS observations, the nuclear EOS has been rigidly constrained. In fact, the observation of the highest NS mass beyond $2M_\odot$ [2–4] ruled several out softer EOSs. For the NS radius, several experimental and observational constraints have been established (for a recent review, see [5]), but there remains significant uncertainties.

In this study, we investigate the dependence of light curves for X-ray bursts on the NS EOS, focusing on the uncertainties of the NS radius. We compare our calculated burst models with the observations of GS 1826–24.

*e-mail: dohi@phys.kyushu-u.ac.jp

2 The methods of multi-zone X-ray burst calculations

Table 1. Physical quantities at the nuclear saturation density for adopted EOSs

EOS	ρ_0 [10^{14} g cm^{-3}]	w_0 [MeV]	K_0 [MeV]	$E_{\rm sym}$ [MeV]	L [MeV]
Togashi	2.66	−16.0	245	30.0	35.0
TM1	2.41	−16.3	281	36.9	111
TM1e	2.41	−16.3	281	31.4	40.0
LS220	2.57	−16.0	220	28.6	73.8

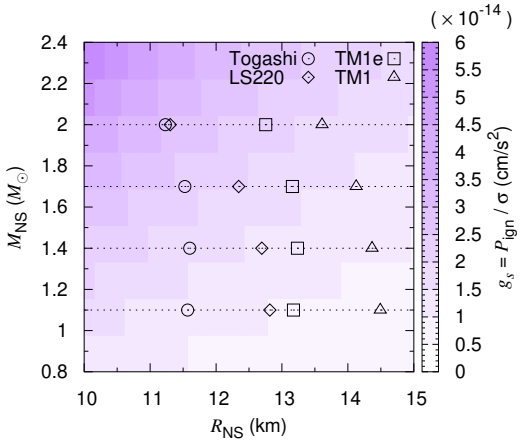

Figure 1. The surface gravity g_s on the mass–radius plane based on the *shell-flash* model. The symbols indicate the values with our adopted EOSs.

To calculate X-ray-burst light curves considering the central NS, we use a one-dimensional general-relativistic stellar-evolution code [6] (hereinafter called *full* multi-zone model). Namely, we follow the thermal evolution of accreting NSs in quasi-hydrostatic equilibrium. To reduce the costs of numerical calculations, we adopt a reduced nuclear-reaction network with 88 nuclei for H or He mixed burning (APRX3 in [7]). For time evolution of H and He mass fractions and energy generation rates, APRX3 reproduces the resulting energy generation rates with a large reaction network with 897 nuclei within the 40% error.

We implement sets of realistic nuclear EOSs of Togashi [8], LS220 [9], TM1e [10], and TM1 [11]. The information of NS EOS such as the pressure and energy density comes from the energy per nucleon $w(\rho_{\rm B}, Y_p)$, where $\rho_{\rm B}$ is the baryon density and Y_p is the proton fraction, which can be expanded around the saturation density ρ_0:

$$w(\rho_{\rm B}, Y_p) = w_0 + \frac{K_0}{18\rho_0^2}(\rho_{\rm B}-\rho_0)^2 + \cdots + \left[E_{\rm sym} + \frac{L}{3\rho_0}(\rho_{\rm B}-\rho_0) + \cdots\right]\left(1-2Y_p\right)^2, \quad (1)$$

where w_0, K_0, $E_{\rm sym}$, and L are, respectively, energy per nucleon, incompressibility, symmetry energy, and its slope at ρ_0. Thus, any EOS can be mostly characterised by the five parameters. For our adopted EOSs, we show their values in Table 1. The important parameter for the NS radius is L, being still uncertain (e.g., [12]). In our EOSs, the TM1 has the largest L value and radius of $R_{1.4}$ = 14.3 km, while the Togashi smallest L value and $R_{1.4}$ = 11.6 km, where

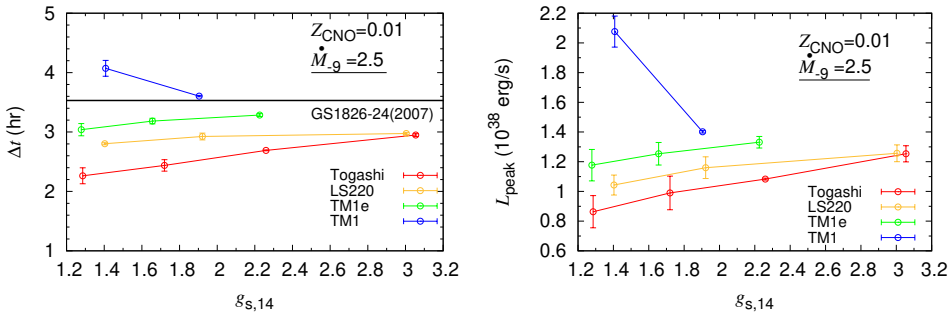

Figure 2. Δt and $L_{\rm peak}$ plotted by $g_{s,14}$ with different EOSs. The horizontal solid line corresponds to the observed value of GS 1826–24 in 2007 [17]. Some burst models are omitted if hydrostatic equilibrium conditions are not achieved.

$R_{1.4}$ is the radius at $M_{\rm NS} = 1.4\ M_\odot$. Thus, the radius is highly different in the range of about 11–14 km, depending on the symmetry energy.

The relation between the mass–radius and burst behavior is roughly expressed by the shell-flush model, assuming the constant pressure during a burning onto the NS [13]:

$$P_{\rm ign} = g_{\rm s}\sigma, \tag{2}$$

where σ is the column depth and $g_{\rm s}$ is the surface gravity, which considers the general relativistic effect. We show the value of g_s in Figure 1. Suppose that $P_{\rm ign}$ is independent of the NS mass and radius, σ is higher with a large-radius EOS. This implies that the observable recurrence time Δt and the peak luminosity $L_{\rm peak}$ should also be higher. The EOS uncertainties affect burst behavior, which should be clarified in full multi-zone X-ray burst models.

Since $P_{\rm ign}$ comes from the heating and cooling processes inside a NS, it should not be a free parameter, unlike the shell-flush model. Many previous studies with multi-zone X-ray-burst models, which cover the only accreted layers, introduce a similar artificial heating parameter Q_b to impose the envelope and crust boundary conditions (e.g., [1]). To treat the internal energy of NS consistently, we consider the conventional crustal heating process [14] and slow neutrino cooling processes, including the modified Urca and bremsstrahlung (e.g., see [15]). Such cooling processes effectively increase $P_{\rm ign}$, because they decrease the overall temperature before the NS becomes very old ($\gtrsim 10^5$ yrs). Therefore, they change the burst behavior from Eq. (2). In the proceeding, however, we simply focus on the EOS dependence, which does not significantly change neutrino luminosity without any enhanced cooling processes.

To focus on the EOS uncertainties, we fix $\dot{M}_{-9} = 2.5$ and $Z_{\rm CNO} = 0.01$ in the proceeding, where $\dot{M}_{-9}$ is the accretion rate normalized by $10^{-9}\ M_\odot\ {\rm yr}^{-1}$ and $Z_{\rm CNO}$ is the initial metalicity. Note that the influence on light curves is crucially important, but the trend of EOS dependence does not change even if other parameters related to the companion are chosen. As the initial model for calculations, we use the steady-state model of accreting NSs (see [16]).

3 Results

In Figure 2, we show the dependence of Δt and $L_{\rm peak}$ on the EOS. As we see, if the radius is smaller, Δt and $L_{\rm peak}$ are lower because the amount of accreted matter is increased due to a stronger gravitational field. It finally shorten the ignition time, and therefore this trend is

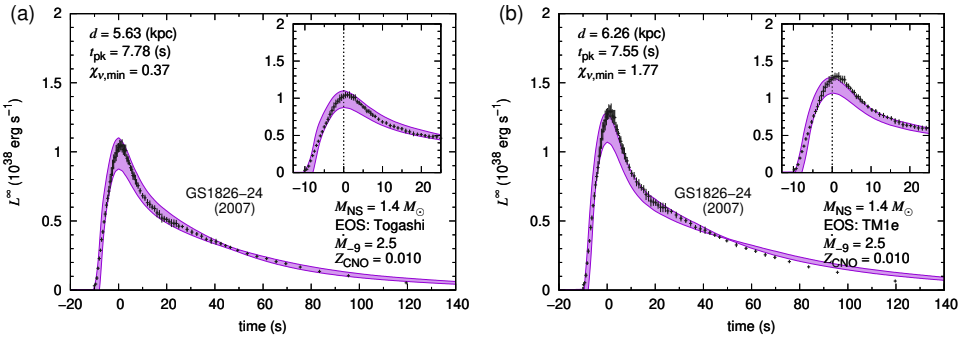

Figure 3. Comparison of calculated averaged burst light curves with observed ones of GS 1826–24 in 2007, assuming $\dot{M}_{-9} = 2.5, Z_{\rm CNO} = 0.01$ and $M_{\rm NS} = 1.4\ M_\odot$: (a) Togashi , (b) TM1e. We set $t = 0$ s at the peak time of light curves and plot within 1σ regions of many burst light curves. The distance including burst anisotropy d, the time after the peak $t_{\rm pk}$, and the minimum χ^2 value $\chi_{\nu,\rm min}$ are also shown.

consistent with the results of shell-flush model. For the Δt, we compare our models with the observation of GS 1826–24 in 2007 [17]. There is no model matching with observed Δt, but if $\dot{M}_{-9}, Z_{\rm CNO}$ and NS mass change, it could be reproduced (see the model of "L2n20Z1" in [7]; $\dot{M}_{-9} = 2.0, Z_{\rm CNO} = 0.01$, LS220 EOS, and $M_{\rm NS} = 1.58\ M_\odot$.).

We show that the comparison with the observed light curve of GS 1826–24 in 2007 in Figure 3. For the TM1e, the peak luminosity is higher than the Togashi due to the fuel amount difference. Thus, the Togashi agrees with the shape of observed light curves, while the TM1e disagrees. The luminosity is too high in large-radius NSs and sometimes reaches the Eddington luminosity. However, GS 1826–24 do not show photospheric radius expansion. Therefore, large-radius EOSs (e.g., TM1) tend to be rejected, although the model comparison highly depends on other input parameters, e.g., $\dot{M}_{-9}$ and $Z_{\rm CNO}$.

4 Conclusion

We study the dependence of the NS EOS on Type-I X-ray burst using multi-zone X-ray-burst models, with an emphasis on the observation of a clocked burster GS 1826–24. We find that Δt and $L_{\rm peak}$ are higher with larger-radius EOSs, whose trend are consistent with the shell-flush model. As a result of the comparison with the observation of GS 1826–24, we also find that larger-radius EOS is unpreferred due to higher luminosities. Since the EOS is related to internal heating and cooling processes, self-consistent burst calculations including the evolution of a NS are necessary. In the burst calculations presented here, we adopt the conventional heating and cooling processes, which should be updated. The more detailed analysis which are done with a series of X-ray burst calculations are shown in the paper [18].

References

[1] Z. Johnston, A. Heger, D.K. Galloway, Mon. Not. Roy. Astron. Soc. **494**, 4576 (2020), `arXiv:1909.07977`
[2] P.B. Demorest *et al.*, Nature **467**, 1081 (2010), `arXiv:1010.5788`
[3] J. Antoniadis *et al.*, Science **340**, 448 (2013), `arXiv:1304.6875`
[4] H.T. Cromartie *et al.*, Nat. Astron. **4**, 72 (2020), `arXiv:1904.06759`

[5] G.F. Burgio, H.J. Schulze, I. Vidaña, J.B. Wei, Prog. Part. Nucl. Phys. **120**, 103879 (2021), arXiv:2105.03747
[6] M.Y. Fujimoto, T. Hanawa, J. Iben, I., M.B. Richardson, Astrophys. J. **278**, 813 (1984)
[7] A. Dohi, M.a. Hashimoto, R. Yamada, Y. Matsuo, M.Y. Fujimoto, Prog. Theor. Exp. Phys. **2020**, 033E02 (2020), arXiv:2001.08367
[8] H. Togashi, K. Nakazato, Y. Takehara, S. Yamamuro, H. Suzuki, M. Takano, Nucl. Phys. A**961**, 78 (2017), arXiv:1702.05324
[9] J.M. Lattimer, D.F. Swesty, Nucl. Phys. A**535**, 331 (1991)
[10] H. Shen, F. Ji, J. Hu, K. Sumiyoshi, Astrophys. J. **891**, 148 (2020), arXiv:2001.10143
[11] H. Shen, H. Toki, K. Oyamatsu, K. Sumiyoshi, Astrophys. J. Suppl. **197**, 20 (2011), arXiv:1105.1666
[12] B.A. Li, B.J. Cai, W.J. Xie, and N.B. Zhang, Univ., **7**, 182 (2021)
[13] M.Y. Fujimoto, T. Hanawa, S. Miyaji, Astrophys. J. **247**, 267 (1981)
[14] P. Haensel, J.L. Zdunik, Astron. Astrophys. **227**, 431 (1990)
[15] A. Dohi, K. Nakazato, M.a. Hashimoto, M. Yasuhide, T. Noda, Prog. Theor. Exp. Phys. **2019**, 113E01 (2019), arXiv:1910.01431
[16] H. Liu, A. Dohi, M.a. Hashimoto, Y. Matsuo, G.L. Lü, T. Noda, Phys. Rev. D**103**, 063009 (2021), arXiv:2102.04012
[17] D.K. Galloway, A.J. Goodwin, L. Keek, Publ. Astron. Soc. Australia. **34**, e019 (2017), arXiv:1703.07485
[18] A. Dohi, N. Nishimura, M. Hashimoto, Y. Matsuo, T. Noda, S. Nagataki, Astrophys. J. **923**, 16 (2021),